Structure of Even-Even $^{218\text{-}230}$Ra Isotopes within the Interacting Boson Approximation Model

Sohair M. Diab

Faculty of Education, Phys. Dept., Ain Shams University, Cairo, Egypt

E-mail: mppe2@yahoo.co.uk

A good description of the excited positive and negative parity states of radium nuclei ($Z = 88$, $N = 130$–142) is achieved using the interacting boson approximation model (IBA-1). The potential energy surfaces, energy levels, parity shift, electromagnetic transition rates $B(E1)$, $B(E2)$ and electric monopole strength $X(E0/E2)$ are calculated for each nucleus. The analysis of the eigenvalues of the model Hamiltonian reveals the presence of an interaction between the positive and negative parity bands. Due to this interaction the $\Delta I = 1$ staggering effect, between the energies of the ground state band and the negative parity state band, is produced including beat patterns.

1 Introduction

The existence of stable octupole deformation in actinide nuclei has encouraged many authors to investigate these nuclei experimentally and theoretically but until now no definitive signatures have been established. Different models have been considered, but none has provided a complete picture of octupole deformation.

Cluster model has been applied to $^{221\text{-}226}$Ra by many authors [1–7]. The intrinsic multipole transition moment and parity splitting were calculated. Also, the half-lives of cluster emission are predicted. In general, cluster model succeeded in reproducing satisfactory the properties of normal deformed ground state and super deformed excited bands in a wide range of even-even nuclei.

A proposed formalism of the collective model [8, 9, 10] have been used in describing the strong parity shift observed in low-lying spectra of ^{224,226}Ra and ^{224,226}Th with octupole deformations together with the fine rotational band structure developed at higher angular momenta. Beat staggering patterns are obtained also for $^{218\text{-}226}$Ra and ^{224,226}Th.

The mean field model [11] and the analytic quadrupole octupole axially symmetric ($AQOA$) model [12] have been applied to ^{224,226}Ra and ^{226}Ra nuclei respectively, and found useful for the predictions of the decay properties where the experimental data are scarce.

$Spdf$ interacting boson model [13] has been applied to the even-even $^{218\text{-}228}$Ra isotopes and an explanation of how the octupole deformation can arise in the rotational limit. The discussion of the properties of the fractional symmetric rigid rotor spectrum [14] and the results of its application to the low excitation energy of the ground state band of $^{214\text{-}224}$Ra show an agreement with the experimental data.

The aim of the present paper is to calculate and analyze the complete spectroscopic properties of the low-lying positive and negative parity excited states in $^{218\text{-}230}$Ra isotopes using IBA-1 Hamiltonian. The potential energy surfaces, levels energy, parity shift, electromagnetic transition rates and electric monopole strength $X(E0/E2)$ are calculated.

2 (IBA-1) model

2.1 Level energies

The IBA-1 model describes the low-lying energy states of the even-even radium nuclei as a system of interacting s-bosons and d-bosons. The π and ν bosons are treated as one boson. Introducing creation $\left(s^\dagger d^\dagger\right)$ and annihilation $\left(s\tilde{d}\right)$ operators for s and d bosons, the most general Hamiltonian [15] which includes one-boson term in boson-boson interaction has been used in calculating the levels energy is:

$$\begin{aligned} H &= EPS \cdot n_d + PAIR \cdot (P \cdot P) + \\ &+ \frac{1}{2}\, ELL \cdot (L \cdot L) + \frac{1}{2}\, QQ \cdot (Q \cdot Q) + \\ &+ 5OCT \cdot (T_3 \cdot T_3) + 5HEX \cdot (T_4 \cdot T_4)\,, \end{aligned} \tag{1}$$

where

$$P \cdot p = \frac{1}{2} \begin{bmatrix} \left\{(s^\dagger s^\dagger)^{(0)}_0 - \sqrt{5}(d^\dagger d^\dagger)^{(0)}_0\right\} x \\ \left\{(ss)^{(0)}_0 - \sqrt{5}(\tilde{d}\tilde{d})^{(0)}_0\right\} \end{bmatrix}^{(0)}_0 , \tag{2}$$

$$L \cdot L = -10\sqrt{3}\left[(d^\dagger \tilde{d})^{(1)} x\, (d^\dagger \tilde{d})^{(1)}\right]^{(0)}_0 , \tag{3}$$

$$Q \cdot Q = \sqrt{5} \begin{bmatrix} \left\{(S^\dagger \tilde{d} + d^\dagger s)^{(2)} - \frac{\sqrt{7}}{2}\,(d^\dagger \tilde{d})^{(2)}\right\} x \\ \left\{(s^\dagger \tilde{d} + +\tilde{d}s)^{(2)} - \frac{\sqrt{7}}{2}\,(d^\dagger \tilde{d})^{(2)}\right\} \end{bmatrix}^{(0)}_0 , \tag{4}$$

$$T_3 \cdot T_3 = -\sqrt{7}\left[(d^\dagger \tilde{d})^{(2)} x\, (d^\dagger \tilde{d})^{(2)}\right]^{(0)}_0 , \tag{5}$$

$$T_4 \cdot T_4 = 3\left[(d^\dagger \tilde{d})^{(4)} x\, (d^\dagger \tilde{d})^{(4)}\right]^{(0)}_0 . \tag{6}$$

nucleus	EPS	$PAIR$	ELL	QQ	OCT	HEX	$E2SD(eb)$	$E2DD(eb)$
$_{218}$Ra	0.3900	0.000	0.0005	−0.0090	0.0000	0.0000	0.2020	−0.5957
$_{220}$Ra	0.3900	0.000	0.0005	−0.0420	0.0000	0.0000	0.1960	−0.5798
$_{222}$Ra	0.0650	0.0000	0.0100	−0.0650	0.0000	0.0000	0.1960	−0.5798
$_{224}$Ra	0.2000	0.0000	0.0060	−0.0450	0.0000	0.0000	0.1640	−0.4851
$_{226}$Ra	0.0700	0.0000	0.0060	−0.0450	0.0000	0.0000	0.1660	−0.4910
$_{228}$Ra	0.0600	0.0000	0.0060	−0.0380	0.0000	0.0000	0.1616	−0.4780
$_{230}$Ra	0.0580	0.0000	0.0060	−0.0502	0.0000	0.0000	0.1560	−0.4615

Table 1. Parameters used in IBA-1 Hamiltonian (all in MeV).

In the previous formulas, n_d is the number of boson; $P{\cdot}P$, $L \cdot L$, $Q \cdot Q$, $T_3 \cdot T_3$ and $T_4 \cdot T_4$ represent pairing, angular momentum, quadrupole, octupole and hexadecupole interactions between the bosons; EPS is the boson energy; and $PAIR$, ELL, QQ, OCT, HEX is the strengths of the pairing, angular momentum, quadrupole, octupole and hexadecupole interactions.

2.2 Transition rates

The electric quadrupole transition operator [15] employed in this study is given by:

$$T^{(E2)} = E2SD \cdot (s^\dagger \tilde{d} + d^\dagger s)^{(2)} + \\ + \frac{1}{\sqrt{5}} E2DD \cdot (d^\dagger \tilde{d})^{(2)} . \tag{7}$$

The reduced electric quadrupole transition rates between $I_i \to I_f$ states are given by

$$B(E_2, I_i - I_f) = \frac{[< I_f \parallel T^{(E_2)} \parallel I_i >]^2}{2I_i + 1} . \tag{8}$$

3 Results and discussion

3.1 The potential energy surface

The potential energy surfaces [16], $V(\beta, \gamma)$, for radium isotopes as a function of the deformation parameters β and γ have been calculated using:

$$\begin{aligned} E_{N_\Pi N_\nu}(\beta, \gamma) &= <N_\pi N_\nu; \beta\gamma\, |H_{\pi\nu}| N_\pi N_\nu; \beta\gamma> = \\ &= \zeta_d(N_\nu N_\pi)\beta^2(1+\beta^2) + \beta^2(1+\beta^2)^{-2} \times \\ &\times \left\{ kN_\nu N_\pi[4 - (\bar{X}_\pi \bar{X}_\nu)\beta \cos 3\gamma] \right\} + \\ &+ \left\{ [\bar{X}_\pi \bar{X}_\nu \beta^2] + N_\nu(N_\nu - 1)\left(\frac{1}{10}c_0 + \frac{1}{7}c_2\right)\beta^2 \right\} , \end{aligned} \tag{9}$$

where

$$\bar{X}_\rho = \left(\frac{2}{7}\right)^{0.5} X_\rho \quad \rho = \pi \text{ or } \upsilon . \tag{10}$$

The calculated potential energy surfaces for radium series of isotopes presented in Fig. 1 show that ^{218}Ra is a vibrational-like nucleus where the deformation β is zero. ^{220}Ra nucleus started to deviate from vibrational-like and a slight prolate deformation appeared. $^{222\text{-}230}$Ra nuclei show more deformation on the prolate and oblate sides, but the deformation on the prolate side is deeper.

3.2 Energy spectra

IBA-1 model has been used in calculating the energy of the positive and negative parity low -lying levels of radium series of isotopes. A comparison between the experimental spectra [17–23] and our calculations, using the values of the model parameters given in Table 1 for the ground and octupole bands, is illustrated in Fig. 2. The agreement between the theoretical and their correspondence experimental values for all the nuclei are slightly higher but reasonable. The most striking is the minimum observed in the negative parity states, Fig. 3, at $N = 136$ which interpreted as ^{224}Ra is the most deformed nucleus in this chain of isotopes.

3.3 Electromagnetic transitions rates

Unfortunately there is no enough measurements of $B(E1)$ or $B(E2)$ rates for these series of nuclei. The only measured $B(E2, 0_1^+ \to 2_1^+)$'s are presented, in Table 2a, for comparison with the calculated values. The parameters $E2SD$ and $E2DD$ used in the present calculations are determined by normalizing the calculated values to the experimentally known ones and displayed in Tables 2a and 2b.

For calculating $B(E1)$ and $B(E2)$ transition rates of intraband and interaband we did not introduce any new parameters. The calculated values some of it are presented in Fig. 4 and Fig. 5 which show bending in the two figures at $N = 136$ which support what we have seen in Fig. 3 as ^{224}Ra is the most octupole deformed nucleus.

3.4 Electric monopole transitions

The electric monopole transitions, $E0$, are normally occurring between two states of the same spin and parity by transferring energy and zero unit of angular momentum. The strength of the electric monopole transition, $X_{if'f}(E0/E2)$,

I_i^+ I_f^+	^{218}Ra	^{220}Ra	^{222}Ra	^{224}Ra	^{226}Ra	^{228}Ra	^{230}Ra
0_1 Exp. 2_1	1.10(20)	———	4.54(39)	3.99(15)	5.15(14)	5.99(28)	——-
0_1 Theor. 2_1	1.1222	2.4356	4.5630	3.9633	5.1943	5.9933	6.6861
2_1 0_1	0.224	0.4871	0.9126	0.7927	1.0389	1.1987	1.3372
2_2 0_1	0.0005	0.0028	0.0001	0.0014	0.0002	0.0001	0.0001
2_2 0_2	0.086	0.2509	0.5978	0.5287	0.7444	0.8878	1.0183
2_3 0_1	0.000	0.0058	0.0001	0.0015	0.0001	0.0001	0.0001
2_3 0_2	0.173	0.0854	0.0141	0.0075	0.0122	0.0122	0.0118
2_3 0_3	0.022	0.0476	0.0001	0.0011	0.0001	0.0000	0.0000
2_4 0_3	0.010	0.1322	0.3662	0.3013	0.5326	0.6481	0.7627
2_4 0_4	0.152	0.0707	0.0006	0.0041	0.0001	0.0000	0.0000
2_2 2_1	0.300	0.0819	0.0003	0.0034	0.0003	0.0003	0.0001
2_3 2_1	0.0001	0.0023	0.0002	0.0022	0.0002	0.0002	0.0001
2_3 2_2	0.088	0.4224	0.0690	0.0730	0.0398	0.0348	0.0302
4_1 2_1	0.368	0.7474	1.2490	1.0973	1.4449	1.6752	1.8756
4_1 2_2	0.0318	0.0337	0.0004	0.0051	0.0004	0.0004	0.0002
4_1 2_3	0.0715	0.0331	0.0000	0.0002	0.0000	0.0000	0.0000
6_1 4_1	0.4194	0.7924	1.2673	1.1380	1.5138	1.7714	1.9970
6_1 4_2	0.0463	0.0270	0.0004	0.0057	0.0005	0.0004	0.0002
6_1 4_3	0.0514	0.0249	0.0001	0.0009	0.0000	0.0000	0.0000
8_1 6_1	0.3749	0.7217	1.626	1.0830	1.4672	1.7430	1.9864
8_1 6_2	0.0529	0.0205	0.0004	0.0051	0.0006	0.0005	0.0002
8_1 6_3	0.0261	0.0170	0.0001	0.0018	0.0001	0.0001	0.0000
10_1 8_1	0.2346	0.5600	0.9737	0.9649	1.3492	1.6406	1.9005
10_1 8_2	0.0553	0.0161	0.0003	0.0041	0.0005	0.0005	0.0002

Table 2a. Values of the theoretical reduced transition probability, $B(E2)$ (in $e^2\, b^2$).

I_i^- I_f^+	^{218}Ra	^{220}Ra	^{222}Ra	^{224}Ra	^{226}Ra	^{228}Ra	^{230}Ra
1_1 0_1	0.0008	0.0605	0.1942	0.1886	0.2289	0.2612	0.3033
1_1 0_2	0.1203	0.0979	0.0222	0.0293	0.0195	0.0190	0.0183
3_1 2_1	0.1117	0.1921	0.3352	0.3301	0.3927	0.4378	0.4937
3_1 2_2	0.0451	0.0325	0.0245	0.0330	0.0243	0.0238	0.0228
3_1 2_3	0.0025	0.0095	0.0001	0.0001	0.0000	0.0000	0.0001
3_1 4_1	0.0015	0.0094	0.0419	0.0458	0.0791	0.0883	0.0926
3_1 4_2	0.0007	0.0040	0.0073	0.0100	0.0099	0.0090	0.0074
5_1 4_1	0.2397	0.3169	0.4358	0.4349	0.5032	0.5493	0.6043
5_1 4_2	0.0531	0.0267	0.0187	0.0260	0.0214	0.0214	0.0205
5_1 4_3	0.0017	0.0027	0.0006	0.0005	0.0002	0.0002	0.0003
7_1 6_1	0.3839	0.4454	0.5349	0.5388	0.6033	0.6476	0.6996
7_1 6_2	0.0476	0.0204	0.0121	0.0187	0.0168	0.0173	0.0169
9_1 8_1	0.5429	0.5785	0.6398	0.6479	0.7041	0.7452	0.7936
9_1 8_2	0.0295	0.0139	0.0070	0.0129	0.0122	0.0131	0.0132

Table 2b. Values of the theoretical reduced transition probability, $B(E1)$ (in $\mu\, e^2 b$).

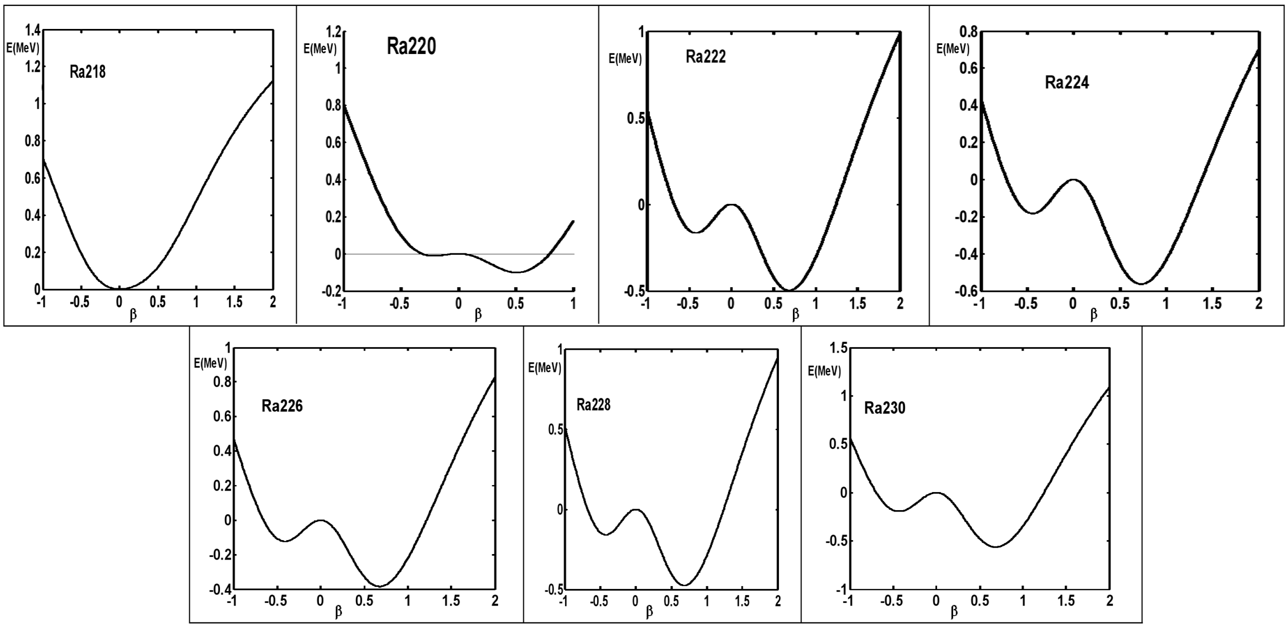

Fig. 1: The potential energy surfaces for $^{218-230}$Ra nuclei.

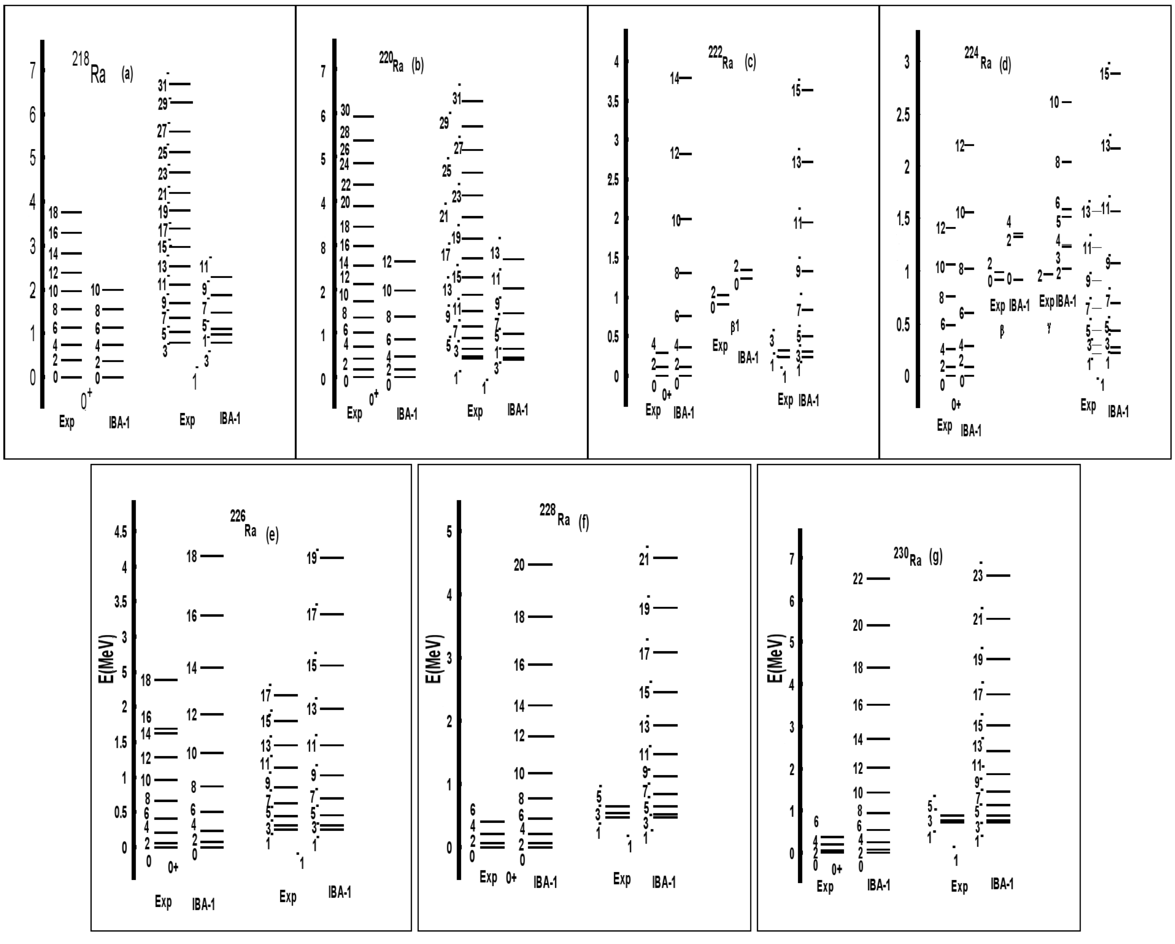

Fig. 2: Comparison between experimental (Exp.) and theoretical (IBA-1) energy levels in $^{218-230}$Ra, (a–g).

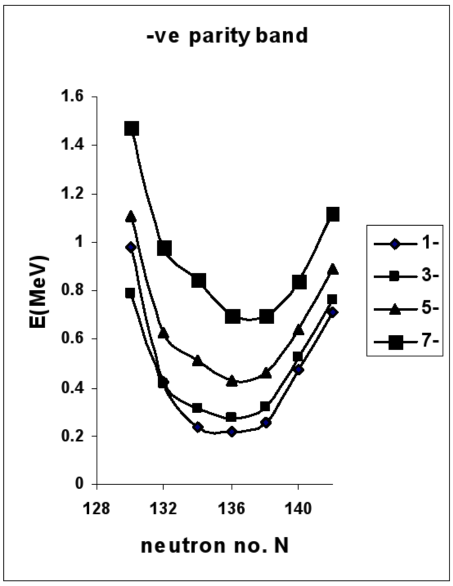

Fig. 3: Energy versus neutron numbers N for the $-ve$ parity band in $^{218\text{-}230}$Ra.

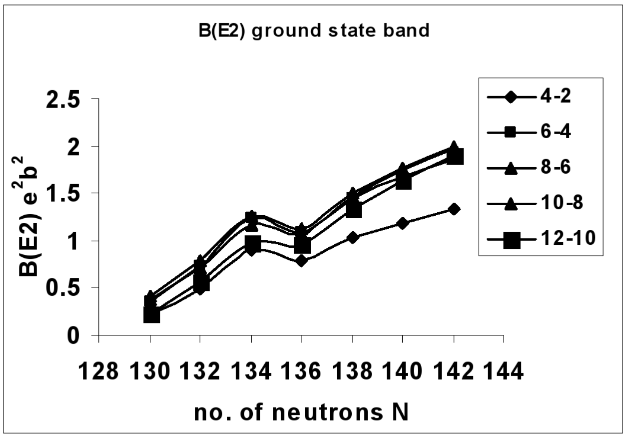

Fig. 4: The calculated $B(E2)$'s for the ground state band of Ra isotopes.

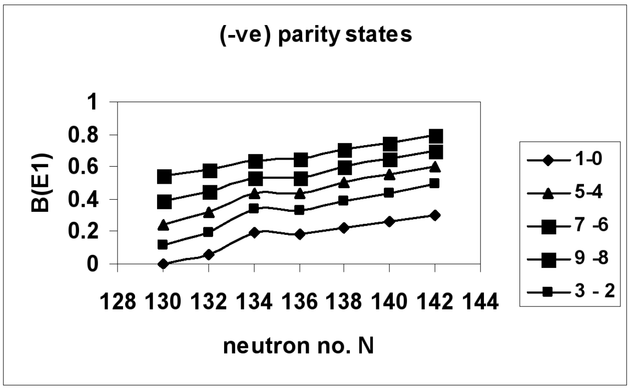

Fig. 5: The calculated $B(E1)$'s for the $(-ve)$ parity band.

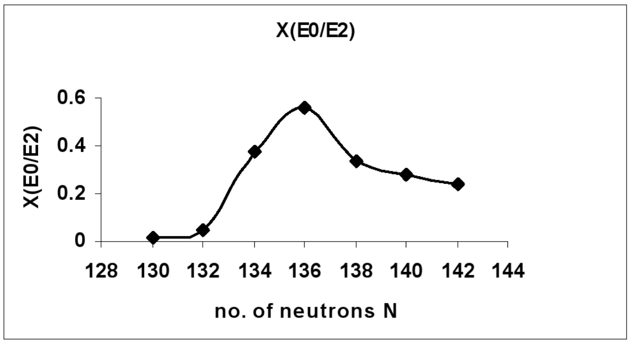

Fig. 6: The calculated $X(E0/E2,\ 2_2^+ \to 0_1^+)$ versus N for $^{218\text{-}230}$Ra isotopes.

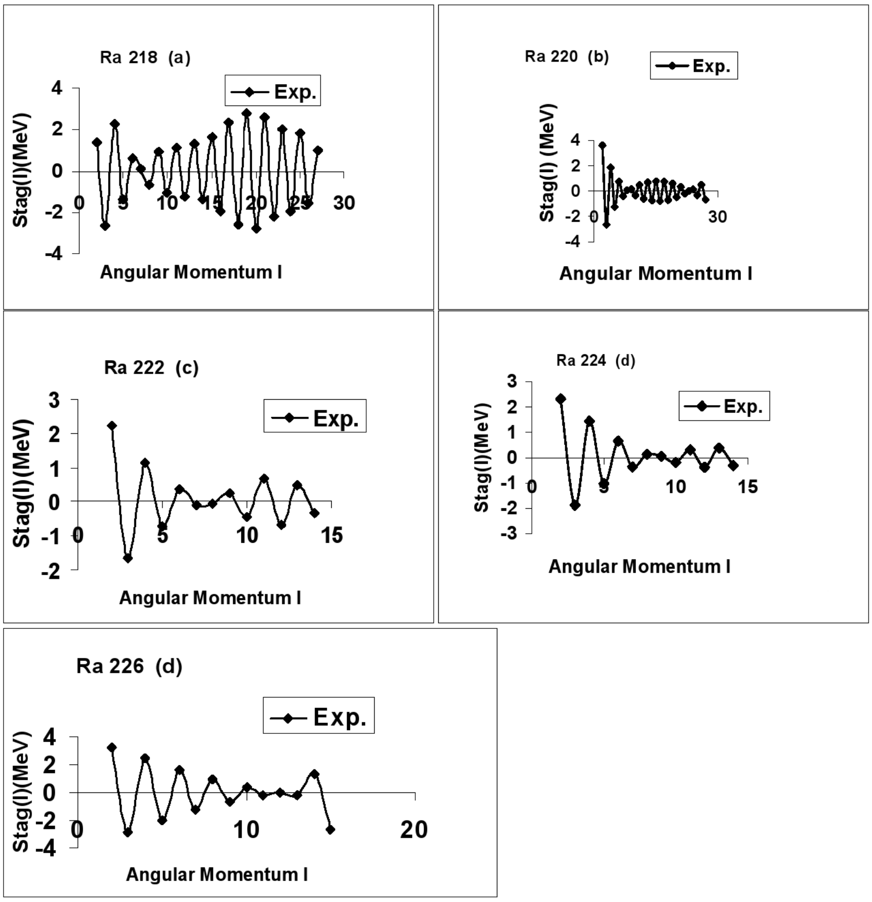

Fig. 7: $\Delta I = 1$, staggering patterns for the ground state and octupole bands of $^{218-230}$Ra isotope.

I_i^+	I_f^+	$I_{f'}^+$	^{218}Ra	^{220}Ra	^{222}Ra	^{224}Ra	^{226}Ra	^{228}Ra	^{230}Ra
0_2	0_1	2_1	0.016	0.046	0.376	0.562	0.335	0.279	0.243
0_3	0_1	2_1	0.125	——	——	0.058	0.081	—-	0.500
0_3	0_1	2_2	0.007	0.058	—-	0.009	0.003	——	0.230
0_3	0_1	2_3	0.015	0.002	—-	0.333	0.005	——	0.0005
0_3	0_2	2_1	—-	——	10.00	1.705	0.702	2.000	9.000
0_3	0_2	2_2	——	0.029	0.008	0.027	0.027	0.189	4.153
0_3	0_2	2_3	———	0.001	——	9.666	0.054	0.049	0.103
0_4	0_1	2_2	0.009	0.008	1.200	—-	1.700	0.391	0.094
0_4	0_1	2_3	0.009	1.000	—-	1.230	0.459	1.636	—-
0_4	0_1	2_4	0.005	0.018	0.027	4.000	1.307	0.129	5.000
0_4	0_2	2_2	0.018	0.042	1.400	——	0.1000	——	0.037
0_4	0_2	2_3	0.019	5.000	——	0.769	0.027	——	——
0_4	0_2	2_4	0.011	0.093	0.031	2.500	0.076	——	2.000
0_4	0_3	2_1	——	——	0.250	—-	0.333	——-	——
0_4	0_3	2_2	—-	——	0.066	——	0.001	——	——
0_4	0_3	2_3	——	——	——	——	0.027	——	——
0_4	0_3	2_4	——	——	0.001	—-	0.076	——	——-

Table 3. Theoretical $X_{if'f}$ $(E0/E2)$ ratios for $E0$ transitions in Ra isotopes.

[24] can be calculated using equations (11, 12) and presented in Table 3. Fig. 6 shows also that ^{224}Ra has strong electric monopole strength than the other radium isotopes which is in agreement with the previous explanations.

$$X_{if'f}(E0/E2) = \frac{B(E0, I_i - I_f)}{B(E2, I_i - I_{'f})}\,, \tag{11}$$

$$X_{if'f}(E0/E2) = (2.54\times10^9)\,A^{3/4} \times \\ \times \frac{E_\gamma^5(\mathrm{MeV})}{\Omega_{KL}}\,\alpha(E2)\,\frac{T_e(E0, I_i - I_f)}{T_e(E_2, I_i - I_{'f})}\,. \tag{12}$$

3.5 The staggering

A presence of an odd-even staggering effect has been observed for $^{218\text{-}230}$Ra series of isotopes [8, 9, 10, 25]. Odd-even staggering patterns between the energies of the ground state band and the $(-ve)$ parity octupole band have been calculated, $\Delta I = 1$, using staggering function as in equations (13, 14) using the available experimental data [17–23].

$$Stag(I) = 6\Delta E(I) - 4\Delta E(I-1) - 4\Delta E(I+1) + \\ + \Delta E(I+2) + \Delta E(I-2)\,, \tag{13}$$

with

$$\Delta E(I) = E(I+1) - E(I)\,. \tag{14}$$

The calculated staggering patterns are illustrated in Fig. 7, where we can see the beat patterns of the staggering behavior which show an interaction between the ground state and the octupole bands.

3.6 Conclusions

The IBA-1 model has been applied successfully to $^{218\text{-}230}$Ra isotopes and we have got:

1. The ground state and octupole bands are successfully reproduced;
2. The potential energy surfaces are calculated and show vibrational characters to ^{218,220}Ra and rotational behavior to $^{222\text{-}230}$Ra isotopes where they are prolate deformed nuclei;
3. Electromagnetic transition rates $B(E1)$ and $B(E2)$ are calculated;
4. The strength of the electric monopole transitions are calculated and show with the other calculated data that ^{224}Ra is the most octupole deformed nucleus;
5. Staggering effect have been observed and beat patterns obtained which show an interaction between the ground state and octupole bands;

Submitted on November 24, 2007
Accepted on December 06, 2007

References

1. Patra S.K.,.Raj K Gupta, Sharma B.K, Stevenson P.D. and Greiner W. *J. Phys. G*, 2007, v. 34, 2073.
2. Adamian G. G., Antonenko N. V., Jolos R. V., Palchikov Yu. V., Scheid W. and Shneidman T. M. *Nucl. Phys. A*, 2004, v. 734, 433.
3. Balasubramaniam M., Kumarasamy S. and Arunachalam N. *Phys. Rev. C*, 2004, v. 70, 017301.
4. Kuklin S. N., Adamian G. G. and Antonenko N. V. *Phys. Rev. C*, 2005, v. 71, 014301.
5. Zhongzhou Ren, Chang Xu and Zaijun Wang. *Phys. Rev. C*, 2004, v. 70, 034304.
6. Buck B., Merchant A. C. and Perez S. M. *Phys. Rev. C*, 2003, v. 68, 024313.
7. Shneidman T. M., Adamian G. G., Antonenko N. V., Jolos R. V. and Scheid W. *Phys. Rev. C*, 2003, v. 67, 014313.
8. Minkov N., Yotov P., Drenska S. and Scheid W. *J. Phys. G*, 2006, v. 32, 497.
9. Bonatsos D., Daskaloyannis C., Drenska S. B., Karoussos N., Minkov N., Raychev P. P. and Roussev R. P. *Phys. Rev. C*, 2000, v. 62, 024301.
10. Minkov N., Drenska S. B., Raychev P. P., Roussev R. P.and Bonatsos D. *Phys. Rev. C*, 2001, v. 63, 044305.
11. Xu F. R. and Pei J. C. *Phys. Lett. B*, 2006, v. 642, 322.
12. Lenis D. and Bonatsos D. *Phys. Lett. B*, 2006, v. 633, 474.
13. Zamfir N. V. and Kusnezov D. *Phys. Rev. C*, 2001, v. 63, 054306.
14. Herrmann R. *J. Phys. G*, 2007, v. 34, 607.
15. Feshband H. and Iachello F. *Ann. Phys.*, 1974, v. 84, 211.
16. Ginocchio J. N and Kirson M. W. *Nucl. Phys. A*, 1980, v. 350, 31.
17. Ashok K. Jain, Balraj Singh. *Nucl. Data Sheets*, 2007, v. 107, 1027.
18. Agda Artna-Cohen. *Nucl. Data Sheets*, 1997, v. 80, 187.
19. Akovali Y. A. *Nucl. Data Sheets*, 1996, v. 77, 271.
20. Agda Artna-Cohen. *Nucl. Data Sheets*, 1997, v. 80, 227.
21. Akovali Y. A. *Nucl. Data Sheets*, 1996, v. 77, 433.
22. Agda Artna-Cohen. *Nucl. Data Sheets*, 1997, v80, 723.
23. Akovali Y.A., *Nucl. Data Sheets*, 1993, v. 69,155.
24. Rasmussen J. O. Theory of $E0$ transitions of spheroidal nuclei. *Nucl. Phys.*, 1960, v. 19, 85.
25. Ganev V. P., Garistov V. P., and Georgieva A. I. *Phys. Rev. C*, 2004, v. 69, 014305.